Dynamical Analysis and Forward Euler Discretisation of an SEIR-Type Epidemic Model Incorporating Vaccination

Fiorentina Abigail, Jonathan Hoseana, and Benny Yong

Abstract—We construct a continuous SEIR-type epidemic model incorporating vaccination, which takes into account the proportion of successful vaccinations and the vaccine's efficacy. We identify a feasible positively-invariant domain for the model and obtain the model's equilibria and basic reproduction number, before establishing sufficient conditions for the equilibria's local asymptotic stability in terms of the obtained basic reproduction number. Subsequently, we construct a discrete analogue of our model using the forward Euler method, and establish sufficient conditions for the local asymptotic stability of the discrete model's equilibria in terms of not only the basic reproduction number but also the discretisation step size. Using the discrete model, we generate and visualise the numerical solutions of our original model in two qualitatively opposite scenarios: disease-free and endemic. A sensitivity analysis reveals that, in both scenarios, reducing inter-individual contacts constitutes a more effective disease-control strategy than accelerating vaccinations.

Index Terms—SEIR, vaccination, discretisation, forward Euler method, sensitivity analysis

I. INTRODUCTION

THE recent COVID-19 pandemic has led to a rapid popularisation of compartmental epidemic models as means for understanding disease dynamics and evaluating intervention strategies. In such models, the population under consideration is divided into several compartments, representing different states associated to the epidemic progression. In one of the simplest compartmental epidemic models, the SIR-type model proposed in 1927 by Kermack and McKendrick [20], the population is divided into three compartments: susceptible (S), infected (I), and removed (R). In various modifications of this model, additional compartments have been introduced. The exposed (E) compartment, in particular, is intended to segregate individuals who have been subjected to the disease but are not yet infectious, giving rise to SEIR-type epidemic models, which capture more accurately the respective disease's incubation period [1], [4], [6], [11], [12], [25], [28], [32], [46], [48], [49], [51], [52], [56], [57]. Furthermore, numerous epidemic models have been constructed to incorporate various intervention strategies, such as vaccination, which has been recognised

Manuscript received July 6, 2025; revised September 2, 2025.

Fiorentina Abigail is a graduate of the Mathematics Programme, Faculty of Science, Parahyangan Catholic University, Bandung, Indonesia (e-mail: fiorentinaabigail02@gmail.com).

Jonathan Hoseana is a researcher at the Center for Mathematics and Society, Faculty of Science, Parahyangan Catholic University, Bandung, Indonesia (corresponding author, e-mail: j.hoseana@unpar.ac.id).

Benny Yong is a researcher at the Center for Mathematics and Society, Faculty of Science, Parahyangan Catholic University, Bandung, Indonesia (e-mail: benny_y@unpar.ac.id).

for its effectiveness in reducing disease transmission [2], [9], [15], [26], [30], [42], [43], [50], [54].

In 1998, Shulgin et al. [42] incorporated two modes of vaccination —constant and pulsed— into a modified Kermack-McKendrick SIR-type model that features demographic factors. Subsequently, in 2002, Lu et al. [29] conducted a similar study using another modified SIR-type Kermack-McKendrick model, which features not only demographic factors but also vertical transmission. Complementarily, SEIR-type epidemic models have been employed in numerous studies with a variety of purposes: to investigate the dynamical behaviour induced by saturated incidence and treatment rates [12], [28], [46], [48], [57], to examine the impact of constant, pulsed, and periodic vaccinations [6], [32], [49], [51], [52], and to simulate the transmission dynamics of COVID-19 in particular regions [1], [4]. Notably, the models employed in such studies are mostly continuous, and the analyses very rarely include the dynamical properties of the model's discretised counterpart, despite it providing a basis for the conducted numerical simulations.

In this paper, we present a modest continuous SEIR-type epidemic model incorporating constant vaccination, along with its discretised counterpart obtained using the forward Euler method [22, sec. 22.3]. To construct the model itself, we assume that vaccinations are administered to individuals upon their recruitment, taking into account both the proportion of successful vaccinations and the vaccine's efficacy. We regard successfully vaccinated recruited individuals as removed, and the remaining recruited individuals as susceptible. We assume that susceptible, exposed, infected, and recovered individuals experience mortality at linear rates, with possibly different proportionality constants. On the whole, our model can be viewed as both a simplified variant of the SEIR-type model constructed by Wintachai and Prathom [51] and a developed variant of the constant-vaccination model constructed by Shulgin et al. [42].

Our work is organised as follows. In the upcoming section II, we construct our continuous SEIR-type model and study its dynamical properties. In particular, we determine the model's basic reproduction number \mathcal{R}_0 , and show that the model possesses a disease-free equilibrium and an endemic equilibrium, which are locally asymptotically stable if $\mathcal{R}_0 < 1$ and if $\mathcal{R}_0 > 1$, respectively. In the subsequent section III, we construct the forward-Euler discretisation of our model, which possesses the same equilibria. We determine sufficient conditions on the discretisation step size that guarantee the local asymptotic stability of the disease-free equilibrium in the case $\mathcal{R}_0 < 1$, and that of the endemic equilibrium in the case $\mathcal{R}_0 > 1$. In section IV, we use our discrete model

to generate numerical solutions of our original continuous model, in two scenarios representing the cases $\mathcal{R}_0 < 1$ and $\mathcal{R}_0 > 1$, respectively. We also conduct a sensitivity analysis in order to determine our model's parameters upon which \mathcal{R}_0 depends most sensitively. In the final section V, we state our conclusions and suggest avenues for further investigation.

II. MODEL CONSTRUCTION AND DYNAMICAL ANALYSIS

In this section, we first construct our SEIR-type model in its continuous form (subsection II-A) and study its solutions' non-negativity and boundedness (subsection II-B). Subsequently, we determine the model's equilibria and basic reproduction number (subsection II-C) and derive conditions for the equilibria's stability in terms of the obtained basic reproduction number (subsection II-D).

A. Model construction

To construct our model, consider a situation where a disease spreads over population in such a way that at any given time, each individual in the population belong to exactly one of the following compartments: susceptible (S), exposed (E), infected (I), and removed (R). We denote by S = S(t), E = E(t), I = I(t), and R = R(t) thenumbers of individuals belonging to each compartment at time $t \ge 0$. Letting b > 0 be the population's recruitment rate, we assume that individuals recruited to the population are vaccinated in a way that the proportion of successful vaccinations and the vaccine's efficacy are given by $v \in [0, 1]$ and $p \in [0,1]$, respectively, so that recruited individuals enter the susceptible compartment at the constant rate of (1-vp) b and the removed compartment at the constant rate of vpb. Next, we assume that susceptible individuals become exposed at a bilinear incidence rate of βSI , where $\beta > 0$ denotes the disease's incidence coefficient, that exposed individuals become infected at a linear rate of αE , where $\alpha > 0$ denotes the disease's incubation coefficient, and that infected individuals become removed at a linear rate of γI , where $\gamma > 0$ denotes the disease's recovery coefficient. Finally, we assume that susceptible, exposed, infected, and removed individuals experience mortality at the linear rates of d_0S , d_1E , d_2I , and d_3R , respectively, where $d_0, d_1, d_2, d_3 > 0$. These assumptions lead to the compartmental diagram shown in Figure 1, and to the following continuous SEIR-type model:

$$\begin{cases} \frac{dS}{dt} = (1 - vp) b - \beta SI - d_0 S, \\ \frac{dE}{dt} = \beta SI - \alpha E - d_1 E, \\ \frac{dI}{dt} = \alpha E - \gamma I - d_2 I, \\ \frac{dR}{dt} = vpb + \gamma I - d_3 R. \end{cases}$$
(1)

The parameters involved in the model (1) are summarised in Table I.

B. Non-negativity and boundedness of solutions

Let us now verify the non-negativity and boundedness of the solutions of our model (1). For this purpose, let (S, E, I, R) = (S(t), E(t), I(t), R(t)) be such a solution,

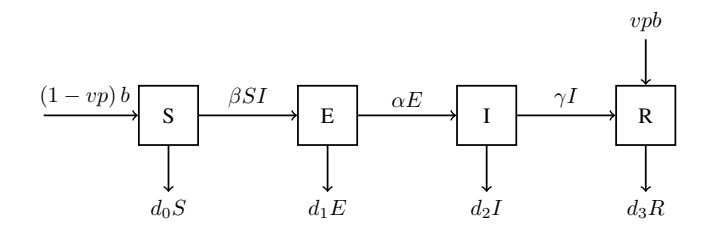


Fig. 1. Compartmental diagram of our model (1).

TABLE I
SUMMARY OF PARAMETERS INVOLVED IN OUR MODEL (1) AND THEIR
VALUES USED IN OUR NUMERICAL SIMULATIONS.

Parameter	Description	Unit	Value for simulation
α	incubation coefficient	1/day	0.02 0.90
β	incidence coefficient	1/(individual × day)	0.01
γ	recovery coefficient	1/day	0.15
v	proportion of successful vaccinations	-	0.50
p	vaccine efficacy	-	0.70
b	recruitment rate	individual/day	2.00
d_0	death coefficient of susceptible individuals	1/day	0.03
d_1	death coefficient of exposed individuals	1/day	0.03
d_2	death coefficient of infected individuals	1/day	0.03
d_3	death coefficient of removed individuals	1/day	0.03
S(0)	initial number of susceptible individuals	individual	100
E(0)	initial number of exposed individuals	individual	1
I(0)	initial number of infected individuals	individual	1
R(0)	initial number of recovered individuals	individual	0

associated to an initial condition $(S(0), E(0), I(0), R(0)) \in \mathbb{R}^4_+$, where $\mathbb{R}_+ = [0, \infty)$. Since at each time $t^* \geqslant 0$ where $S(t^*) = 0$ we have that

$$\frac{\mathrm{d}S}{\mathrm{d}t}\Big|_{t=t^*} = (1 - vp) \, b > 0,$$

by the first equation in (1), implying that $S(t) \ge 0$ for all $t \ge 0$. Similarly, one deduces that $E(t) \ge 0$, $I(t) \ge 0$, and $R(t) \ge 0$ for all $t \ge 0$.

Next, suppose that N = N(t) = S(t) + E(t) + I(t) + R(t). Adding the four equations in (1) gives

$$\frac{\mathrm{d}N}{\mathrm{d}t} = b - d_0 S - d_1 E - d_2 I - d_3 R \leqslant b - dN,$$

i.e.,

$$\frac{\mathrm{d}N}{\mathrm{d}t} + dN \leqslant b,$$

where $d = \min\{d_0, d_1, d_2, d_3\}$. Multiplying both sides by e^{dt} gives

$$\frac{\mathrm{d}}{\mathrm{d}t} \left[\mathrm{e}^{dt} N(t) \right] \leqslant b \mathrm{e}^{dt} = \frac{\mathrm{d}}{\mathrm{d}t} \left[\frac{b}{d} \mathrm{e}^{dt} + N(0) - \frac{b}{d} \right].$$

It follows that for all $t \ge 0$ we have

$$e^{dt}N(t) \leqslant \frac{b}{d}e^{dt} + N(0) - \frac{b}{d},$$

i.e.,

$$N(t) \leqslant \frac{b}{d} + \left[N(0) - \frac{b}{d} \right] \mathrm{e}^{-dt} \xrightarrow{t \to \infty} \frac{b}{d}$$

completing the proof of the following theorem.

Theorem 1. The sets \mathbb{R}^4_+ and

$$\left\{ (S, E, I, R) \in \mathbb{R}_+^4 : S + E + I + R \leqslant \frac{b}{d} \right\} \subseteq \mathbb{R}_+^4,$$

where $d = \min\{d_0, d_1, d_2, d_3\}$, are positively invariant under the model (1).

C. Equilibria and basic reproduction number

Let us continue the dynamical analysis of our model (1) by determining the model's equilibria [41], [44]. These are the solutions of the system

$$\begin{cases}
0 = (1 - vp) b - \beta SI - d_0 S, \\
0 = \beta SI - \alpha E - d_1 E, \\
0 = \alpha E - \gamma I - d_2 I, \\
0 = vpb + \gamma I - d_3 R.
\end{cases}$$
(2)

The third equation gives

$$E = \frac{\gamma + d_2}{\alpha} I. \tag{3}$$

Substituting (3) into the system's second equation gives

$$0 = \beta SI - \alpha \left(\frac{\gamma + d_2}{\alpha} I \right) - d_1 \left(\frac{\gamma + d_2}{\alpha} I \right)$$
$$= I \left[\beta S - \frac{(\alpha + d_1)(\gamma + d_2)}{\alpha} \right],$$

which leads to two cases.

In the first case, I=0. Substituting this to (3) gives E=0, and to the system's first and fourth equations gives

$$S = \frac{(1 - vp) b}{d_0} \qquad \text{and} \qquad R = \frac{vpb}{d_3}.$$

We thus obtain our model's disease-free equilibrium

$$\mathcal{E}_0 = (S_0, E_0, I_0, R_0) = \left(\frac{(1 - vp)b}{d_0}, 0, 0, \frac{vpb}{d_3}\right). \quad (4)$$

In the second case, we have that

$$S = \frac{(\alpha + d_1)(\gamma + d_2)}{\alpha \beta}.$$

Substituting this into the first equation in (2) gives

$$I = \frac{\alpha (1 - vp) b}{(\alpha + d_1) (\gamma + d_2)} - \frac{d_0}{\beta}.$$
 (5)

Substituting this into (3) gives

$$E = \frac{(1 - vp) b}{\alpha + d_1} - \frac{d_0 (\gamma + d_2)}{\alpha \beta}.$$

Finally, substituting (5) into the fourth equation in (2) gives

$$R = \frac{vpb}{d_3} + \frac{\gamma}{d_3} \left[\frac{\alpha (1 - vp) b}{(\alpha + d_1) (\gamma + d_2)} - \frac{d_0}{\beta} \right].$$

This leads to the model's endemic equilibrium

$$\mathcal{E}_1 = (S_1, E_1, I_1, R_1), \tag{6}$$

where

$$\begin{split} S_1 &= \frac{\left(\alpha + d_1\right)\left(\gamma + d_2\right)}{\alpha\beta}, \\ E_1 &= \frac{\left(1 - vp\right)b}{\alpha + d_1} - \frac{d_0\left(\gamma + d_2\right)}{\alpha\beta}, \\ I_1 &= \frac{\alpha\left(1 - vp\right)b}{\left(\alpha + d_1\right)\left(\gamma + d_2\right)} - \frac{d_0}{\beta}, \\ R_1 &= \frac{vpb}{d_3} + \frac{\gamma}{d_3} \left[\frac{\alpha\left(1 - vp\right)b}{\left(\alpha + d_1\right)\left(\gamma + d_2\right)} - \frac{d_0}{\beta} \right]. \end{split}$$

Let us now apply van den Driessche and Watmough's nextgeneration approach [10], [31] to determine the model's basic reproduction number, taking as infectious compartments our exposed and infected compartments. By our model (1), the numbers of individuals in each of these compartments evolve according to the equations

$$\begin{split} \frac{\mathrm{d}E}{\mathrm{d}t} &= \mathcal{F}_1\left(S, E, I, R\right) - \mathcal{V}_1\left(S, E, I, R\right), \\ \frac{\mathrm{d}I}{\mathrm{d}t} &= \mathcal{F}_2\left(S, E, I, R\right) - \mathcal{V}_2\left(S, E, I, R\right), \end{split}$$

where

$$\mathcal{F}_1(S, E, I, R) = \beta SI,$$

$$\mathcal{F}_2(S, E, I, R) = 0,$$

$$\mathcal{V}_1(S, E, I, R) = (\alpha + d_1) E,$$

$$\mathcal{V}_2(S, E, I, R) = -\alpha E + (\gamma + d_2) I.$$

Next, constructing the matrices

$$\mathbf{F} = \begin{bmatrix} \frac{\mathrm{d}\mathcal{F}_{1}}{\mathrm{d}E} \left(\mathcal{E}_{0} \right) & \frac{\mathrm{d}\mathcal{F}_{1}}{\mathrm{d}I} \left(\mathcal{E}_{0} \right) \\ \frac{\mathrm{d}\mathcal{F}_{2}}{\mathrm{d}E} \left(\mathcal{E}_{0} \right) & \frac{\mathrm{d}\mathcal{F}_{2}}{\mathrm{d}I} \left(\mathcal{E}_{0} \right) \end{bmatrix} = \begin{bmatrix} 0 & \frac{\beta \left(1 - vp \right)b}{d_{0}} \\ 0 & 0 \end{bmatrix}$$

and

$$\mathbf{V} = \begin{bmatrix} \frac{\mathrm{d}\mathcal{V}_1}{\mathrm{d}E} \left(\mathcal{E}_0 \right) & \frac{\mathrm{d}\mathcal{V}_1}{\mathrm{d}I} \left(\mathcal{E}_0 \right) \\ \frac{\mathrm{d}\mathcal{V}_2}{\mathrm{d}E} \left(\mathcal{E}_0 \right) & \frac{\mathrm{d}\mathcal{V}_2}{\mathrm{d}I} \left(\mathcal{E}_0 \right) \end{bmatrix} = \begin{bmatrix} \alpha + d_1 & 0 \\ -\alpha & \gamma + d_2 \end{bmatrix},$$

one finds that the next-generation matrix of our model (1) is given by

$$\mathbf{FV}^{-1} = \begin{bmatrix} 0 & \frac{\beta (1 - vp) b}{d_0} \\ 0 & 0 \end{bmatrix} \begin{bmatrix} \alpha + d_1 & 0 \\ -\alpha & \gamma + d_2 \end{bmatrix}^{-1}$$
$$= \begin{bmatrix} \frac{\alpha \beta (1 - vp) b}{d_0 (\alpha + d_1) (\gamma + d_2)} & \frac{\beta (1 - vp) b}{d_0 (\alpha + d_1)} \\ 0 & 0 \end{bmatrix}.$$

Thus, the model's basic reproduction number —the spectral radius of the above matrix— is given by

$$\mathcal{R}_0 = \frac{\alpha\beta (1 - vp) b}{d_0 (\alpha + d_1) (\gamma + d_2)}$$

By straightforward algebraic manipulations, one may rewrite the coordinates of the model's endemic equilibrium (6) in terms of \mathcal{R}_0 as

$$S_{1} = \frac{(1 - vp) b}{d_{0} \mathcal{R}_{0}}, \qquad I_{1} = \frac{d_{0} (\mathcal{R}_{0} - 1)}{\beta},$$

$$E_{1} = \frac{d_{0} (\gamma + d_{2}) (\mathcal{R}_{0} - 1)}{\alpha \beta}, \quad R_{1} = \frac{vpb}{d_{3}} + \frac{\gamma d_{0} (\mathcal{R}_{0} - 1)}{\beta d_{3}}.$$

This makes it apparent that, while the disease-free equilibrium (4) exists in \mathbb{R}^4_+ for all parameter values, the endemic equilibrium (6) exists if and only if $\mathcal{R}_0 \geqslant 1$. Let us summarise our findings in this and previous subsections in the following theorem.

Theorem 2. The model (1) in its positively invariant domain \mathbb{R}_4^+ possesses the disease-free equilibrium

$$\mathcal{E}_0 = (S_0, E_0, I_0, R_0) = \left(\frac{(1 - vp)b}{d_0}, 0, 0, \frac{vpb}{d_3}\right), \quad (7)$$

which exists for all parameter values, and the endemic equilibrium

$$\mathcal{E}_1 = (S_1, E_1, I_1, R_1), \tag{8}$$

$$\begin{split} S_1 &= \frac{\left(1 - vp\right)b}{d_0 \mathcal{R}_0}, \qquad I_1 = \frac{d_0 \left(\mathcal{R}_0 - 1\right)}{\beta}, \\ E_1 &= \frac{d_0 \left(\gamma + d_2\right) \left(\mathcal{R}_0 - 1\right)}{\alpha \beta}, \quad R_1 = \frac{vpb}{d_3} + \frac{\gamma d_0 \left(\mathcal{R}_0 - 1\right)}{\beta d_3}, \end{split}$$

which exists if and only if $\mathcal{R}_0 \geqslant 1$, where

$$\mathcal{R}_0 = \frac{\alpha\beta (1 - vp) b}{d_0 (\alpha + d_1) (\gamma + d_2)} \tag{9}$$

is the model's basic reproduction number.

D. Local asymptotic stability of equilibria

Let us next study the local asymptotic stability of the disease-free and endemic equilibria \mathcal{E}_0 and \mathcal{E}_1 using the Jacobian matrix of our model (1

$$\mathbf{J}(S, E, I, R) = \begin{bmatrix} -d_0 - \beta I & 0 & -\beta S & 0\\ \beta I & -\alpha - d_1 & \beta S & 0\\ 0 & \alpha & -\gamma - d_2 & 0\\ 0 & 0 & \gamma & -d_3 \end{bmatrix}. (10)$$

Evaluating this at our model's disease-free equilibrium

$$\mathcal{E}_{0} = \left(\frac{(1-vp)b}{d_{0}}, 0, 0, \frac{vpb}{d_{3}}\right)$$
$$= \left(\frac{(\alpha+d_{1})(\gamma+d_{2})}{\alpha\beta}\mathcal{R}_{0}, 0, 0, \frac{vpb}{d_{2}}\right)$$

$$\mathbf{J}\left(\mathcal{E}_{0}\right) = \begin{bmatrix} -d_{0} & 0 & -\frac{\left(\alpha+d_{1}\right)\left(\gamma+d_{2}\right)}{\alpha}\mathcal{R}_{0} & 0\\ 0 & -\alpha-d_{1} & \frac{\left(\alpha+d_{1}\right)\left(\gamma+d_{2}\right)}{\alpha}\mathcal{R}_{0} & 0\\ 0 & \alpha & -\gamma-d_{2} & 0\\ 0 & 0 & \gamma & -d_{3} \end{bmatrix}$$

The characteristic polynomial $|\lambda \mathbf{I} - \mathbf{J}(\mathcal{E}_0)|$ of this matrix is

$$\begin{vmatrix} \lambda + d_0 & 0 & \frac{(\alpha + d_1)(\gamma + d_2)}{\alpha} \mathcal{R}_0 & 0 \\ 0 & \lambda + \alpha + d_1 & -\frac{(\alpha + d_1)(\gamma + d_2)}{\alpha} \mathcal{R}_0 & 0 \\ 0 & -\alpha & \lambda + \gamma + d_2 & 0 \\ 0 & 0 & -\gamma & \lambda + d_3 \end{vmatrix}$$
$$= (\lambda + d_0)(\lambda + d_3) p(\lambda),$$

where

$$p(\lambda) = \begin{vmatrix} \lambda + \alpha + d_1 & -\frac{(\alpha + d_1)(\gamma + d_2)}{\alpha} \mathcal{R}_0 \\ -\alpha & \lambda + \gamma + d_2 \end{vmatrix}$$
$$= \lambda^2 + \mathcal{A}_1 \lambda + \mathcal{A}_2,$$

with

$$\mathcal{A}_1 = \alpha + d_1 + \gamma + d_2,$$

$$\mathcal{A}_2 = (\alpha + d_1)(\gamma + d_2)(1 - \mathcal{R}_0).$$

The eigenvalues of $\mathbf{J}(\mathcal{E}_0)$ thus comprise $-d_0$, $-d_3$, and the two roots of the polynomial $p(\lambda)$. If $\mathcal{R}_0 < 1$, then $\mathcal{A}_1 > 0$ and $A_2 > 0$, so that the Routh-Hurwitz criterion [5, sec. 4.5] implies that all eigenvalues of $\mathbf{J}(\mathcal{E}_0)$ have negative real parts. If $\mathcal{R}_0 = 1$, then the origin is a root of $p(\lambda)$. If $\mathcal{R}_0 > 1$, then p(0) < 0, and since $p(\lambda) \xrightarrow{\lambda \to \infty} \infty$, the intermediate value theorem guarantees that $p(\lambda)$ possesses a positive real root. Our conclusion is the following theorem.

Theorem 3. The disease-free equilibrium \mathcal{E}_0 of the model (1) is locally asymptotically stable if $\mathcal{R}_0 < 1$, is non-hyperbolic if $\mathcal{R}_0 = 1$, and is unstable if $\mathcal{R}_0 > 1$.

Next, evaluating the Jacobian matrix (10) at our model's endemic equilibrium \mathcal{E}_1 gives

acobian matrix of our model (1):
$$\mathbf{J}\left(S,E,I,R\right) = \begin{bmatrix} -d_0 - \beta I & 0 & -\beta S & 0\\ \beta I & -\alpha - d_1 & \beta S & 0\\ 0 & \alpha & -\gamma - d_2 & 0\\ 0 & 0 & \gamma & -d_3 \end{bmatrix}. \quad \text{(10)} \quad \mathbf{J}\left(\mathcal{E}_1\right) = \begin{bmatrix} -d_0\mathcal{R}_0 & 0 & -\frac{(\alpha+d_1)\left(\gamma+d_2\right)}{\alpha} & 0\\ d_0\left(\mathcal{R}_0-1\right) - \alpha - d_1 & \frac{(\alpha+d_1)\left(\gamma+d_2\right)}{\alpha} & 0\\ 0 & \alpha & -\gamma - d_2 & 0\\ 0 & 0 & \gamma & -d_3 \end{bmatrix}.$$
 Evaluating this at our model's disease-free equilibrium

The characteristic polynomial $|\lambda \mathbf{I} - \mathbf{J}(\mathcal{E}_1)|$ of this matrix is

where

$$q(\lambda) = \begin{vmatrix} \lambda + d_0 \mathcal{R}_0 & 0 & \frac{(\alpha + d_1)(\gamma + d_2)}{\alpha} \\ -d_0 (\mathcal{R}_0 - 1) \lambda + \alpha + d_1 & -\frac{(\alpha + d_1)(\gamma + d_2)}{\alpha} \\ 0 & -\alpha & \lambda + \gamma + d_2 \end{vmatrix}$$

$$= \begin{vmatrix} \lambda + d_0 \mathcal{R}_0 & 0 & \frac{(\alpha + d_1)(\gamma + d_2)}{\alpha} \\ \lambda + d_0 & \lambda + \alpha + d_1 & 0 \\ 0 & -\alpha & \lambda + \gamma + d_2 \end{vmatrix}$$

$$= -(\alpha + d_1)(\gamma + d_2)(\lambda + d_0)$$

$$+ (\lambda + \gamma + d_2)[\lambda^2 + (\alpha + d_1 + d_0 \mathcal{R}_0)\lambda + d_0 \mathcal{R}_0 (\alpha + d_1)]$$

$$= \lambda^3 + \mathcal{B}_1 \lambda^2 + \mathcal{B}_2 \lambda + \mathcal{B}_3,$$

with

$$\begin{split} \mathcal{B}_{1} &= \alpha + d_{1} + \gamma + d_{2} + d_{0}\mathcal{R}_{0}, \\ \mathcal{B}_{2} &= \left(\alpha + d_{1} + d_{0}\mathcal{R}_{0}\right)\left(\gamma + d_{2}\right) + d_{0}\mathcal{R}_{0}\left(\alpha + d_{1}\right) \\ &- \left(\alpha + d_{1}\right)\left(\gamma + d_{2}\right) \\ &= d_{0}\mathcal{R}_{0}\left(\alpha + d_{1} + \gamma + d_{2}\right), \\ \mathcal{B}_{3} &= d_{0}\mathcal{R}_{0}\left(\alpha + d_{1}\right)\left(\gamma + d_{2}\right) - d_{0}\left(\alpha + d_{1}\right)\left(\gamma + d_{2}\right) \\ &= d_{0}\left(\mathcal{R}_{0} - 1\right)\left(\alpha + d_{1}\right)\left(\gamma + d_{2}\right). \end{split}$$

Suppose that $\mathcal{R}_0 > 1$. Notice that $\mathcal{B}_1 > 0$ and $\mathcal{B}_3 > 0$. Moreover, noticing that

$$C_1 = \mathcal{B}_1 - \alpha - d_1 = \gamma + d_2 + d_0 \mathcal{R}_0 > 0$$

and

$$C_2 = \mathcal{B}_2 - d_0 \mathcal{R}_0 (\gamma + d_2) = d_0 \mathcal{R}_0 (\alpha + d_1) > 0,$$

one computes that

$$\mathcal{B}_{1}\mathcal{B}_{2} - \mathcal{B}_{3} = (\mathcal{C}_{1} + \alpha + d_{1}) \left[\mathcal{C}_{2} + d_{0}\mathcal{R}_{0} (\gamma + d_{2}) \right] - d_{0} (\mathcal{R}_{0} - 1) (\alpha + d_{1}) (\gamma + d_{2}) = \mathcal{C}_{1} + d_{0}\mathcal{R}_{0} (\gamma + d_{2}) \mathcal{C}_{1} + (\alpha + d_{1}) \mathcal{C}_{2} + d_{0} (\alpha + d_{1}) (\gamma + d_{2}) > 0.$$

The Routh-Hurwitz criterion [5, sec. 4.5] thus implies that the four eigenvalues of $\mathbf{J}(\mathcal{E}_1)$ possess negative real parts. On the other hand, if $\mathcal{R}_0=1$, then the origin is a root of $q(\lambda)$. If $\mathcal{R}_0>1$, then q(0)<0, and since $q(\lambda)\xrightarrow{\lambda\to\infty}\infty$, the intermediate value theorem guarantees that $q(\lambda)$ possesses a positive real root. We have therefore proved the following theorem.

Theorem 4. The endemic equilibrium \mathcal{E}_1 of the model (1) is unstable if $\mathcal{R}_0 < 1$, is non-hyperbolic if $\mathcal{R}_0 = 1$, and is locally asymptotically stable if $\mathcal{R}_0 > 1$.

III. DISCRETISATION

To facilitate our numerical simulations, in this section we apply the forward Euler method to construct a discretised version of our model (1) that possesses the same equilibria \mathcal{E}_0 and \mathcal{E}_1 , and determine sufficient conditions on the discretisation step size under which \mathcal{E}_0 is locally asymptotically stable in the case of $\mathcal{R}_0 < 1$ and \mathcal{E}_1 is locally asymptotically stable in the case of $\mathcal{R}_0 > 1$. To carry out the discretisation,

we first fix a step size $\Delta > 0$ and define the time steps $t_i = i\Delta t$ for every $i \in \{0, 1, \ldots\}$. Next, we define the time-evolving approximants $\overline{S}_i \approx S\left(t_i\right)$, $\overline{E}_i \approx E\left(t_i\right)$, $\overline{I}_i \approx I\left(t_i\right)$, and $\overline{R}_i \approx R\left(t_i\right)$ governed by the recursion

$$\begin{cases}
\overline{S}_{i+1} = \overline{S}_i + \left[(1 - vp) b - d_0 \overline{S}_i - \beta \overline{S}_i \overline{I}_i \right] \Delta t, \\
\overline{E}_{i+1} = \overline{E}_i + \left[\beta \overline{S}_i \overline{I}_i - (\alpha + d_1) \overline{E}_i \right] \Delta t, \\
\overline{I}_{i+1} = \overline{I}_i + \left[\alpha \overline{E}_i - (\gamma + d_2) \overline{I}_i \right] \Delta t, \\
\overline{R}_{i+1} = \overline{R}_i + \left(vpb + \gamma \overline{I}_i - d_3 \overline{R}_i \right) \Delta t,
\end{cases} (11)$$

with $(\overline{S}_0, \overline{E}_0, \overline{I}_0, \overline{R}_0) = (S(0), E(0), I(0), R(0))$. Clearly, the discrete model (11) possesses the same equilibria \mathcal{E}_0 and \mathcal{E}_1 as our continuous model (1). The Jacobian $\overline{\mathbf{J}}(\overline{S}, \overline{E}, \overline{I}, \overline{R})$ of the discrete model (11) reads

$$\begin{bmatrix} 1 - \left(d_0 + \beta \overline{I}\right) \Delta t & 0 & -\beta \overline{S} \Delta t & 0\\ \beta \overline{I} \Delta t & 1 - \left(\alpha + d_1\right) \Delta t & \beta \overline{S} \Delta t & 0\\ 0 & \alpha \Delta t & 1 - \left(\gamma + d_2\right) \Delta t & 0\\ 0 & 0 & \gamma \Delta t & 1 - d_3 \Delta t \end{bmatrix}.$$

The discrete model's Jacobian $\overline{\mathbf{J}}(\mathcal{E}_0)$ at the disease-free equilibrium \mathcal{E}_0 has the characteristic polynomial

$$|\lambda \mathbf{I} - \overline{\mathbf{J}}(\mathcal{E}_0)| = (\lambda - 1 + d_0 \Delta t) (\lambda - 1 + d_3 \Delta t) \overline{p}(\lambda),$$

where

$$\overline{p}(\lambda) = \begin{vmatrix} \lambda - 1 + (\alpha + d_1) \Delta t & -\frac{(\alpha + d_1)(\gamma + d_2)}{\alpha} \mathcal{R}_0 \Delta t \\ -\alpha \Delta t & \lambda - 1 + (\gamma + d_2) \Delta t \end{vmatrix}$$

$$= \lambda^2 + \overline{A}_1 \lambda + \overline{A}_2$$

with

$$\overline{\mathcal{A}}_1 = -2 + (\alpha + d_1 + \gamma + d_2) \Delta t,$$

$$\overline{\mathcal{A}}_2 = 1 - (\alpha + d_1 + \gamma + d_2) \Delta t$$

$$+ (\alpha + d_1) (\gamma + d_2) (1 - \mathcal{R}_0) (\Delta t)^2.$$

Suppose that $\mathcal{R}_0 < 1$. We seek a sufficient condition for the local asymptotic stability of the disease-free equilibrium \mathcal{E}_0 . First, the real eigenvalues $1-d_0\Delta t$ and $1-d_3\Delta t$ lie inside the unit circle if and only if $\Delta t < 2/d_0$ and $\Delta t < 2/d_3$. Next, the Schur-Cohn criterion [13, sec. 5.1] guarantees that the other two eigenvalues also lie inside the unit circle provided that $|\overline{\mathcal{A}}_1| < 1 + \overline{\mathcal{A}}_2 < 2$. The second inequality is equivalent to

$$\Delta t < \frac{\alpha + d_1 + \gamma + d_2}{(\alpha + d_1)(\gamma + d_2)(1 - \mathcal{R}_0)},\tag{12}$$

whereas the first inequality is equivalent to $1 + \overline{A}_1 + \overline{A}_2 > 0$ and $1 - \overline{A}_1 + \overline{A}_2 > 0$. While the former is a tautology, the latter reads

$$0 < (\alpha + d_1) (\gamma + d_2) (1 - \mathcal{R}_0) (\Delta t)^2 - 2 (\alpha + d_1 + \gamma + d_2) \Delta t + 4$$

which can be rewritten as

$$\begin{split} & \left[\Delta t - \frac{\alpha + d_1 + \gamma + d_2}{\left(\alpha + d_1\right)\left(\gamma + d_2\right)\left(1 - \mathcal{R}_0\right)} \right]^2 \\ & > \frac{\left(\alpha + d_1 + \gamma + d_2\right)^2 - 4\left(\alpha + d_1\right)\left(\gamma + d_2\right)\left(1 - \mathcal{R}_0\right)}{\left(\alpha + d_1\right)^2\left(\gamma + d_2\right)^2\left(1 - \mathcal{R}_0\right)^2}. \end{split}$$

If the numerator of the expression on right-hand side is negative, then the inequality is a tautology. Otherwise, knowing that (12) must be satisfied, the inequality is equivalent to

$$\Delta t < \frac{\alpha + d_1 + \gamma + d_2 - \sqrt{\mathcal{K}}}{(\alpha + d_1)(\gamma + d_2)(1 - \mathcal{R}_0)},$$

where

$$\mathcal{K} = (\alpha + d_1 + \gamma + d_2)^2 - 4(\alpha + d_1)(\gamma + d_2)(1 - \mathcal{R}_0).$$

Consequently, we have the following theorem.

Theorem 5. Suppose that $\mathcal{R}_0 < 1$. The disease-free equilibrium \mathcal{E}_0 of the discrete model (11) is locally asymptotically stable if

$$\Delta t < \min \left\{ \frac{2}{d_0}, \frac{2}{d_3}, \frac{\alpha + d_1 + \gamma + d_2 - \sqrt{\max{\{\mathcal{K}, 0\}}}}{(\alpha + d_1)(\gamma + d_2)(1 - \mathcal{R}_0)} \right\},$$

where

$$\mathcal{K} = (\alpha + d_1 + \gamma + d_2)^2 - 4(\alpha + d_1)(\gamma + d_2)(1 - \mathcal{R}_0).$$

On the other hand, the discrete model's Jacobian $\overline{\mathbf{J}}(\mathcal{E}_1)$ at the endemic equilibrium \mathcal{E}_1 has the characteristic polynomial

$$|\lambda \mathbf{I} - \overline{\mathbf{J}}(\mathcal{E}_1)| = (\lambda - 1 + d_3 \Delta t) \overline{q}(\lambda),$$

where

$$q(\lambda) = \lambda^3 + \overline{\mathcal{B}}_1 \lambda^2 + \overline{\mathcal{B}}_2 \lambda + \overline{\mathcal{B}}_3,$$

with

$$\overline{\mathcal{B}}_{1} = -3 + (\alpha + d_{1} + \gamma + d_{2} + d_{0}\mathcal{R}_{0}) \Delta t,
\overline{\mathcal{B}}_{2} = 3 - 2 (\alpha + d_{1} + \gamma + d_{2} + d_{0}\mathcal{R}_{0}) \Delta t
+ d_{0}\mathcal{R}_{0} (\alpha + d_{1} + \gamma + d_{2}) (\Delta t)^{2},
\overline{\mathcal{B}}_{3} = 1 - (\alpha + d_{1} + \gamma + d_{2} + d_{0}\mathcal{R}_{0}) \Delta t
+ d_{0}\mathcal{R}_{0} (\alpha + d_{1} + \gamma + d_{2}) (\Delta t)^{2}
- d_{0} (\mathcal{R}_{0} - 1) (\alpha + d_{1}) (\gamma + d_{2}) (\Delta t)^{3}.$$

Suppose that $\mathcal{R}_0>1$. We seek a sufficient condition for the local asymptotic stability of the endemic equilibrium \mathcal{E}_1 . First, the real eigenvalue $1-d_3\Delta t$ lies inside the unit circle if and only if $\Delta t<2/d_3$. Next, the Schur-Cohn criterion [13, sec. 5.1] guarantees that the other three eigenvalues also lie inside the unit circle provided that $\left|\overline{\mathcal{B}}_1+\overline{\mathcal{B}}_3\right|<1+\overline{\mathcal{B}}_2$ and $\left|\overline{\mathcal{B}}_2-\overline{\mathcal{B}}_1\overline{\mathcal{B}}_3\right|<1-\overline{\mathcal{B}}_3^2$. The first inequality is equivalent to

$$1+\overline{\mathcal{B}}_1+\overline{\mathcal{B}}_2+\overline{\mathcal{B}}_3>0\quad\text{and}\quad 1-\overline{\mathcal{B}}_1+\overline{\mathcal{B}}_2-\overline{\mathcal{B}}_3>0,$$

where the former is a tautology. The following theorem thus follows.

Theorem 6. Suppose that $\mathcal{R}_0 > 1$. The endemic equilibrium \mathcal{E}_1 of the discrete model (11) is locally asymptotically stable if $\Delta t < 2/d_3$, $1 - \overline{\mathcal{B}}_1 + \overline{\mathcal{B}}_2 - \overline{\mathcal{B}}_3 > 0$, and $\left| \overline{\mathcal{B}}_2 - \overline{\mathcal{B}}_1 \overline{\mathcal{B}}_3 \right| < 1 - \overline{\mathcal{B}}_3^2$.

IV. NUMERICAL SIMULATIONS AND SENSITIVITY ANALYSIS

In this section, we utilise our discrete model (11) to generate numerical solutions of our continuous model (1) in two scenarios characterised by two sets of parameter values presented in Table I. The two sets of parameter values are made to differ only on the value of the disease's incubation coefficient, so that the lower incubation coefficient lead to a disease-free scenario $\mathcal{R}_0 < 1$ (subsection IV-A), while the higher incubation coefficient lead to an endemic scenario $\mathcal{R}_0 > 1$ (subsection IV-B). For each scenario, we shall visualise and describe the dynamical behaviour of the generated numerical solution, before conducting a sensitivity analysis of the basic reproduction number with respect to the existing parameters, in order to determine the parameter upon which the basic reproduction number depends most sensitively (subsection IV-C).

A. A disease-free scenario

Our disease-free scenario is represented by the parameter values presented in Table I with $\alpha=0.02$, for which the formulae (9) and (7) lead to $\mathcal{R}_0\approx 0.96<1$ and $\mathcal{E}_0=(S_0,E_0,I_0,R_0)\approx (43.33,0,0,23.33)$, respectively. Let us now specify a value of the discretisation step size Δt that guarantees the desired dynamical consistency: the local asymptotic stability of the disease-free equilibrium \mathcal{E}_0 . Direct computation shows that the upper bound for Δt provided by Theorem 5 evaluates to approximately 8.75. Choosing $\Delta t=1.00<8.75$ and carrying out 800 iterations, we obtain the numerical solution $\left(\left(\overline{S}_i,\overline{E}_i,\overline{I}_i,\overline{R}_i\right)\right)_{i=0}^{800}$ visualised in the left panel of Figure 2. As expected, the solution converges to the disease-free equilibrium \mathcal{E}_0 .

More specifically, we see that the number of susceptible individuals starts at a relatively large value but decreases rapidly at the beginning of the epidemic, due to the initial spread of the infection. Over time, it converges to its equilibrium value $S_0 \approx 43.33$. Meanwhile, the number of exposed individuals begins at a small value, experiences an initial slight increase, but eventually vanishes, indicating that the spread of the infection has terminated, so that $E_0 = 0$ individuals are exposed in the long term. Similarly, the number of infected individuals, which also starts at a low value, shows a slight increase due to the spread of the infection, before decreasing significantly to its equilibrium value $I_0 = 0$, signifying that the infection has been controlled, with no new cases emerging in the long term. By contrast, the number of recovered individuals increases gradually from zero as infected individuals recover and gain immunity. In the long term, where the epidemic has effectively ended, the number of recovered individuals remains in the vicinity of its equilibrium value $R_0 \approx 23.33$.

B. An endemic scenario

Let us now turn to our endemic scenario, which is represented by the parameter values presented in Table I with $\alpha=0.90$. In this scenario, using (9) and (8), one computes that $\mathcal{R}_0\approx 2.33>1$ and $\mathcal{E}_1=(S_1,E_1,I_1,R_1)\approx (18.60,0.80,3.99,43.28)$. To verify that the value of the discretisation step size selected in the previous scenario,

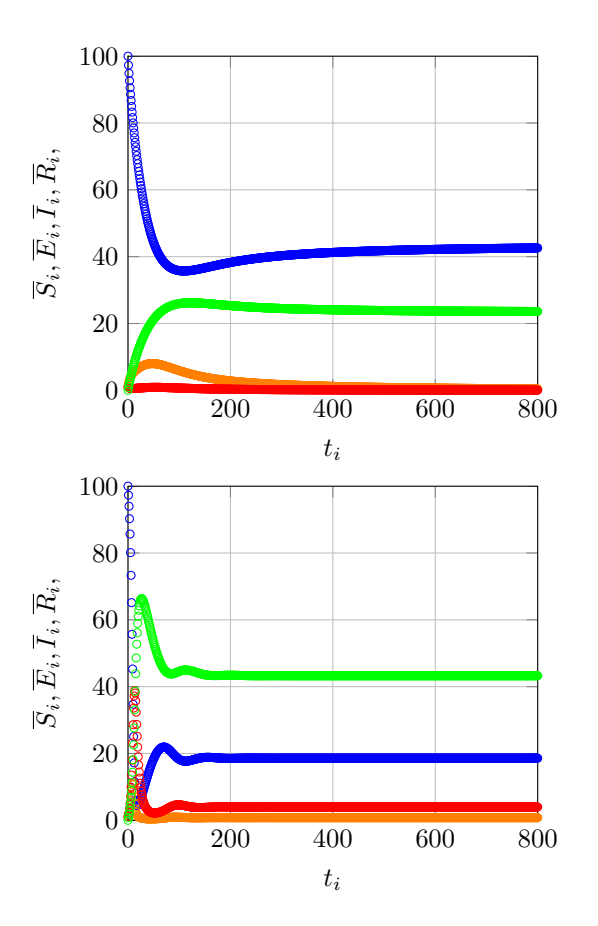


Fig. 2. Plots of the points (t_i, \overline{S}_i) (blue), (t_i, \overline{E}_i) (amber), (t_i, \overline{I}_i) (red), and (t_i, \overline{R}_i) (green) for $i \in \{0, \dots, 800\}$ in our disease-free scenario (left) and in our endemic scenario (right).

 $\Delta t=1.00$, also satisfies the sufficient condition prescribed in Theorem 6, we compute that $2/d_3\approx 66.67$ and

$$\overline{\mathcal{B}}_1 = -1.82, \quad \overline{\mathcal{B}}_2 = -0.72, \quad \text{and} \quad \overline{\mathcal{B}}_3 = -0.11,$$

so that

$$1 - \overline{\mathcal{B}}_1 + \overline{\mathcal{B}}_2 - \overline{\mathcal{B}}_3 \approx 3.65 > 0$$

and

$$\left|\overline{\mathcal{B}}_2 - \overline{\mathcal{B}}_1\overline{\mathcal{B}}_3\right| \approx 0.52 < 0.99 \approx 1 - \overline{\mathcal{B}}_3^2.$$

Utilising, therefore, the same values of discretisation step size and number of iterations, we obtain the numerical solution $((\overline{S}_i, \overline{E}_i, \overline{I}_i, \overline{R}_i))_{i=0}^{800}$ visualised in the right panel of Figure 2, which —as expected— converges to the endemic equilibrium \mathcal{E}_1 .

More specifically, the number of susceptible individuals, which starts at the same relatively large value as in our disease-free scenario, experiences a sharper decline due to the rapid infection spread in the beginning of the epidemic. Over time, the number converges to a lower equilibrium value than in the disease-free condition: $S_1 \approx 18.60$, signifying that a considerable portion of the population is infected. On the other hand, the number of exposed individuals, which starts at a small value, undergoes an initial sharp increase towards a peak, before declining towards its equilibrium value $E_1 \approx 0.80$. This implies that, at the equilibrium state, individuals belonging to the exposed compartment still exist, despite the number remaining constant as opposed to surging as in the beginning of the epidemic. Meanwhile, the number of infected individuals, which also begins at a

TABLE II The values of $\Upsilon_p^{\mathcal{R}_0}$ for all $p\in\{\alpha,\beta,\gamma,v,p,b,d_0,d_1,d_2,d_3\}$ in our disease-free and endemic scenarios.

Sensitivity index	Value in disease-free scenario	Value in endemic scenario
$\Upsilon_{lpha}^{\mathcal{R}_0}$	0.600	0.032
$\Upsilon^{\mathcal{R}_0}_{eta}$	1.000	1.000
$\Upsilon^{\mathcal{R}_0}_{\gamma}$	-0.833	-0.833
$\Upsilon_v^{\mathcal{R}_0}$	-0.538	-0.538
$\Upsilon_p^{\mathcal{R}_0}$	-0.538	-0.538
$\Upsilon_b^{\mathcal{R}_0}$	1.000	1.000
$\Upsilon^{\mathcal{R}_0}_{d_0}$	-1.000	-1.000
$\Upsilon_{d_1}^{\mathcal{R}_0}$	-0.600	-0.032
$\Upsilon^{\mathcal{R}_0}_{d_2}$	-0.166	-0.166
$\Upsilon^{\mathcal{R}_0}_{d_3}$	0.000	0.000

small value, increases rapidly towards a peak that is higher than that in the disease-free scenario. Following the peak, the number of infected individuals decreases and converges to its equilibrium value $I_1 \approx 3.99$. Thus, the disease does not disappear entirely but remains in the population, with a constant number of infected individuals in the long term. Finally, the number of recovered individuals, which also starts at zero as in our disease-free scenario, increases significantly before converging non-monotonically towards its notably large equilibrium value $R_1 \approx 43.28$.

C. Sensitivity analysis

To gain insight on appropriate strategies to maintain a disease-free state and to resolve an endemic state, let us conduct a sensitivity analysis of our model's basic reproduction number \mathcal{R}_0 with respect to the involved parameters $P \in \{\alpha, \beta, \gamma, v, p, b, d_0, d_1, d_2, d_3\}$. The expression (9) implies a differentiable dependence of \mathcal{R}_0 upon all parameters P, thereby allowing the computation of the sensitivity index

$$\Upsilon_P^{\mathcal{R}_0} = \frac{\partial \mathcal{R}_0}{\partial P} \cdot \frac{P}{\mathcal{R}_0}$$

of \mathcal{R}_0 with respect to P, which estimates the ratio of the relative change in \mathcal{R}_0 to the relative change in P [31, p. 139]. For example,

$$\Upsilon_{\alpha}^{\mathcal{R}_0} = \frac{\partial \mathcal{R}_0}{\partial \alpha} \cdot \frac{\alpha}{\mathcal{R}_0} = \frac{d_1}{\alpha + d_1}.$$

Substituting the parameter values in Table I gives $\Upsilon_{\alpha}^{\mathcal{R}_0} \approx 0.60$ in the disease-free scenario and $\Upsilon_{\alpha}^{\mathcal{R}_0} \approx 0.03$ in the endemic scenario. Carrying out a similar computation for each parameter $P \in \{\alpha, \beta, \gamma, v, p, b, d_0, d_1, d_2, d_3\}$, we obtain the values of $\Upsilon_{P}^{\mathcal{R}_0}$ presented in Table II.

Table II reveals that, in both scenarios, our model's basic reproduction number \mathcal{R}_0 depends most sensitively upon the disease's incidence coefficient β and the population's recruitment rate b, whose increases lead to an increase in \mathcal{R}_0 , and upon the death coefficient of the susceptible individuals d_0 , whose increase leads to a decrease in \mathcal{R}_0 . Of note is that neither the proportion of successful vaccination v and the vaccine's efficacy p nor correspond to particularly large absolute sensitivity index values. Since interventions manipulating the population's recruitment rate or the susceptible

individuals' death coefficient might be undesirable, as an appropriate strategy both to maintain a disease-free state and to resolve an endemic state, we recommend the reduction of inter-individual contacts, such as through social distancing, use of masks, self-isolations, and enforcement of adequate hygiene-related protocols.

V. CONCLUSIONS AND FUTURE RESEARCH

We have constructed a continuous SEIR-type epidemic model involving vaccination, which takes into account both the proportion of successful vaccinations and the vaccine's efficacy. We have studied the non-negativity and boundedness of the model's solutions, determined the model's equilibria and basic reproduction number, and studied the stability of the equilibria. We have also applied the forward Euler method to construct a discrete version of our model, which possesses the same equilibria. We have established sufficient conditions on the discretisation step size that ensure the local asymptotic stability of each equilibrium in the relevant case characterised by the basic reproduction number. Finally, we have used our discrete model to generate numerical solutions of our original continuous model in two qualitatively different scenarios represented by two sets of parameter values. In both scenarios, we have also conducted a sensitivity analysis, which reveals that an effective strategy both to maintain a disease-free state and to resolve an endemic state is to not to accelerate vaccinations but to reduce inter-individual contacts.

In future research, one could firstly study the global asymptotic stability of our model's equilibria using Lyapunov functions [31, sec. 7.3]. One could also investigate whether our model could be fitted satisfactorily to empirical data associated with a real-world epidemic, such as COVID-19. For this purpose, one could employ machine-learning methods such as neural networks [3], [40] or Bayesian inference [8], [27], [37] to generate error-minimising estimates for the values of the involved parameters, and possibly evaluate the model's performance in making predictions. Furthermore, one could modify the model by incorporating, for instance, ongoing vaccinations of individuals belonging to the various compartments with possibly different rates [51], vertical transmission [29], quarantined individuals [35], [36], [38], [39], [54], hospitalised individuals [18], [19], [24], [54], and heterogeneity of the population [21], [45]. One could also extend the model by taking into account multiple strains of the spreading disease [16], [23], [47], [53] and apply the model to design a health-and-life insurance policy for individuals in the population under consideration [7], [14], [17], [18], [33], [34], [55].

REFERENCES

- [1] M. Aakash, C. Gunasundari, and Q. M. Al-Mdallal, "Mathematical modeling and simulation of SEIR model for COVID-19 outbreak: A case study of Trivandrum," Frontiers in Applied Mathematics and Statistics, vol. 9, 1124897, 2023.
- [2] A. Abidemi, M. I. A. Aziz, and R. Ahmad, "The impact of vaccination, individual protection, treatment and vector controls on dengue," Engineering Letters, vol. 27, no. 3, pp613-622, 2019.
- [3] M. J. Ahmad and K. Günel, "Can neural networks estimate parameters in epidemiology models using real observed data?," Applied Intelligence, vol. 55, no. 2, 133, 2025.
- [4] S. K. Al-Harbi and S. M. Al-Tuwairqi, "Modeling the effect of lockdown and social distancing on the spread of COVID-19 in Saudi Arabia," PLoS ONE, vol. 17, no. 4, e0265779, 2022.

- [5] L. J. S. Allen, An Introduction to Mathematical Biology, Pearson, New Jersey, 2007.
- [6] R. T. Alqahtani and A. Yusuf, "Development and analysis of a SEIR model for COVID-19 epidemic with vaccination and nonsingular kernel," Fractals, vol. 30, no. 1, 2240040, 2022.
- [7] F. Atatalab, A. T. P. Najafabadi, and M. Zokaei, "Designing an epidemic health insurance," Journal of Mathematics and Modeling in Finance, vol. 5, no. 1, pp121-135, 2025.
- [8] F. C. Coelho, C. T. Codeco, and M. G. M. Gomes, "A Bayesian framework for parameter estimation in dynamical models," PLoS ONE, vol. 6, no. 5, e19616, 2011.
- [9] Y. Chakir, "Global approximate solution of SIR epidemic model with constant vaccination strategy," Chaos, Solitons and Fractals, vol. 169, 113323, 2023.
- [10] P. van den Driessche and J. Watmough, "Reproduction numbers and sub-threshold endemic equilibria for compartmental models of disease transmission," Mathematical Biosciences, vol. 180, no. 1-2, pp29-48, 2002.
- [11] W. J. Du, S. Qin, J. G. Zhang, and J. N. Yu, "Dynamical behavior and bifurcation analysis of SEIR epidemic model and its discretization," IAENG International Journal of Applied Mathematics, vol. 47, no. 1, pp1-8, 2017.
- [12] B. Dubey, A. Putra, P. K. Srivastava, and U. S. Dubey, "Modeling and analysis of an SEIR model with different types of nonlinear treatment rates," Journal of Biological Systems, vol. 21, no. 3, 1350023, 2013.
- [13] S. Elaydi, An Introduction to Difference Equations, 3rd edition, Springer, New York, 2005.
- [14] R. H. Feng and J. Garrido, "Actuarial applications of epidemic models," North American Actuarial Journal, vol. 15, no. 1, pp112-136, 2011.
- [15] E. C. Gabrick, E. L. Brugnago, S. L. T. de Souza, K. C. Iarosz, J. D. Szezech, R. L. Viana, I. L. Caldas, A. M. Batista, and J. Kurths, "Impact of periodic vaccination in SEIRS seasonal model," Chaos: An Interdisciplinary Journal of Nonlinear Science, vol. 34, no. 1, 013137, 2024
- [16] S. Gupta, Rupali, Y. K. Rajoria, and G. P. Sahu, "Mathematical modelling on dynamics of multi-variant SARS-CoV-2 virus: Estimating delta and omicron variant impact on COVID-19," IAENG International Journal of Applied Mathematics, vol. 55, no. 1, pp180-188, 2025.
- [17] D. Hainaut, "An actuarial approach for modeling pandemic risk," Risks, vol. 9, no. 1, 3, 2021.
- [18] J. Hoseana, F. Kusnadi, G. Stephanie, L. Loanardo, and C. Wijaya, "Design and financial analysis of a health insurance based on an SIHtype epidemic model," Journal of Mathematics and Computer Science, vol. 38, no. 2, pp160-178, 2025.
- [19] C. Jia, X. Wang, and Y. Chen, "Complex dynamics of an SIHR epidemic model with variable hospitalization rate depending on unoccupied hospital beds," Mathematics and Computers in Simulation, vol. 229, pp706-724, 2025.
- [20] W. O. Kermack and A. G. McKendrick, "A contribution to the mathematical theory of epidemics," Proceedings of the Royal Society of London, vol. 115, no. 772, pp700-721, 1927.
- [21] S. Klemm and L. Ravera, "On SIR-type epidemiological models and population heterogeneity effects," Physica A: Statistical Mechanics and its Applications, vol. 624, 128928, 2023.
- [22] Q. Kong, T. Siauw, and A. Bayen, Python Programming and Numerical Methods: A Guide for Engineers and Scientists, Academic Press, London, 2021.
- [23] M. A. Kuddus and A. K. Paul, "Global dynamics of a two-strain disease model with amplification, nonlinear incidence and treatment," Iranian Journal of Science, vol. 47, no. 1, pp259-274, 2023.
- [24] C. Legarreta, M. De la Sen, and S. Alonso-Quesada, "On the properties of a newly susceptible, non-seriously infected, hospitalized, and recovered subpopulation epidemic model," Mathematics, vol. 12, no. 2, 245, 2024.
- [25] G. Li and Z. Jin, "Global stability of a SEIR epidemic model with infectious force in latent, infected and immune period," Chaos, Solitons and Fractals, vol. 25, no. 5, pp1177-1184, 2005.
- [26] C. Li and J. Lu, "Novel corona virus disease dynamical models with pulse vaccination," Results in Physics, vol. 53, 107028, 2023.
- [27] N. J. Linden, B. Kramer, and P. Rangamani, "Bayesian parameter estimation for dynamical models in systems biology," PLoS ONE, vol. 19, no. 10, e1011041, 2023.
- [28] J. Liu, "Bifurcation analysis for a delayed SEIR epidemic model with saturated incidence and saturated treatment function," Journal of Biological Dynamics, vol. 13, no. 1, pp461-480, 2019.
- [29] Z. Lu, X. Chi, and L. Chen, "The effect of constant and pulse vaccination on SIR epidemic model with horizontal and vertical transmission," Mathematical and Computer Modelling, vol. 36, no. 9-10, pp1039-1057, 2002.

- [30] Y. Ma and X. Zuo, "Stability analysis of SIRS model considering pulse vaccination and elimination disturbance," Journal of Mathematics, vol. 2024, no. 1, 6617911, 2024.
- [31] M. Martcheva, An Introduction to Mathematical Epidemiology, Springer, New York, 2015.
- [32] I. A. Moneim, "An SEIR model with infectious latent and a periodic vaccination strategy," Mathematical Modelling and Analysis, vol. 26, no. 2, pp236-252, 2021.
- [33] H. S. Nam, "Mathematical and actuarial analysis on a deterministic SEIR model," Global Journal of Pure and Applied Mathematics, vol. 18, no. 2, pp453-464, 2022.
- [34] C. I. Nkeki and G. O. S. Ekhaguere, "Some actuarial mathematical models for insuring the susceptibles of a communicable disease," International Journal of Financial Engineering, vol. 7, no. 2, 2050014, 2020.
- [35] T. Odagaki, "Analysis of the outbreak of COVID-19 in Japan by SIQR model," Infectious Disease Modelling, vol. 5, pp691-698, 2020.
- [36] T. Odagaki, "Exact properties of SIQR model for COVID-19," Physica A: Statistical Mechanics and its Applications, vol. 564, 125564, 2021.
- [37] Y. Ota and N. Mizutani, "Estimating parameters in mathematical model for societal booms through Bayesian inference approach," Mathematical and Computational Applications, vol. 25, no. 3, 42, 2020.
- [38] C. M. A. Pinto, J. A. T. Machado, C. Burgos-Simón, "Modified SIQR model for the COVID-19 outbreak in several countries," Mathematical Methods in the Applied Sciences, vol. 47, no. 5, pp3273-3288, 2024.
- [39] R. Ramesh and G. A. Joseph, "The optimal control methods for the Covid-19 pandemic model's precise and practical SIQR mathematical model," IAENG International Journal of Applied Mathematics, vol. 54, no. 8, pp1657-1672, 2024.
- [40] V. S. H. Rao and M. N. Kumar, "Estimation of the parameters of an infectious disease model using neural networks," Nonlinear Analysis: Real World Applications, vol. 11, no. 3, pp1810-1818, 2010.
- [41] R. C. Robinson, An Introduction to Dynamical Systems: Continuous and Discrete, 2nd edition, American Mathematical Society, Rhode Island, 2012.
- [42] B. Shulgin, L. Stone, and Z. Agur, "Pulse vaccination strategy in the SIR epidemic model," Bulletin of Mathematical Biology, vol. 60, no. 6, pp1123-1148, 1998.
- [43] L. Stone, B. Shulgin, and Z. Agur, "Theoretical examination of the pulse vaccination policy in the SIR epidemic model," Mathematical and Computer Modelling, vol. 31, no. 4-5, pp207-215, 2000.
- [44] S. H. Strogatz, Nonlinear Dynamics and Chaos, 2nd edition, CRC Press, Boca Raton, 2018.
- [45] M. Sun and X. Fu, "Competitive dual-strain SIS epidemiological models with awareness programs in heterogeneous networks: Two modeling approaches," Journal of Mathematical Biology, vol. 87, no. 1, 14, 2023.
- [46] C. Sun, Y. Lin, and S. Tang, "Global stability of an special SEIR epidemic model with nonlinear incidence rates," Chaos, Solitons and Fractals, vol. 33, no. 1, pp290-297, 2007.
- [47] S. K. Tithi, A. K. Paul, and M. A. Kuddus, "Mathematical investigation of a two-strain disease model with double dose vaccination control policies," Results in Physics, vol. 53, 106930, 2023.
- [48] S. Umdekar, P. K. Sharma, and S. Sharma, "An SEIR model with modified saturated incidence rate and Holling type II treatment function," Computational and Mathematical Biophysics, vol. 11, no. 1, 20220146, 2023.
- [49] L. Wang and R. Xu, "Global stability of an SEIR epidemic model with vaccination," International Journal of Biomathematics, vol. 9, no. 6, 1650082, 2016.
- [50] Y. Wang, S. Zhai, M. Du, and P. Zhao, "Dynamic behaviour of multistage epidemic model with imperfect vaccine," IAENG International Journal of Applied Mathematics, vol. 52, no. 4, pp1052-1060, 2022.
- [51] P. Wintachai and K. Prathom, "Stability analysis of SEIR model related to efficiency of vaccines for COVID-19 situation," Heliyon, vol. 7, no. 4, e06812, 2021.
- [52] P. J. Witbooi, S. M. Vyambwera, and M. U. Nsuami, "Control and elimination in an SEIR model for the disease dynamics of COVID-19 with vaccination," AIMS Mathematics, vol. 8, no. 4, pp8144-8161, 2023
- [53] H. Wu, L. Zhang, H. L. Li, and Z. Teng, "Stability analysis and optimal control on a multi-strain coinfection model with amplification and vaccination," Results in Physics, vol. 50, 106556, 2023.
- [54] B. Yong, J. Hoseana, and L. Owen, "From pandemic to a new normal: Strategies to optimise governmental interventions in Indonesia based on an SVEIQHR-type mathematical model," Infectious Disease Modelling, vol. 7, no. 3, pp346-363, 2022.
- [55] C. Zhai, P. Chen, Z. Jin, and T. K. Siu, "Epidemic modelling and actuarial applications for pandemic insurance: A case study of Victoria,

- Australia," Annals of Actuarial Science, vol. 18, no. 2, pp242-269, 2024
- [56] C. Zhang, "Supporting decision-making for COVID-19 outbreaks with the modified SEIR model," IAENG International Journal of Computer Science, vol. 48, no. 1, pp86-95, 2021.
- [57] J. Zhang, J. Jia, and X. Song, "Analysis of an SEIR epidemic model with saturated incidence and saturated treatment function," The Scientific World Journal, vol. 2014, no. 1, 910421, 2014.